TITLE PAGE

Title

Novel complex cavity for second-harmonic subterahertz gyrotrons: a tradeoff between engineering tolerance and mode selection

Author information

Vitalii I. Shcherbinin[1,2] (0000-0002-9879-208X)
Tetiana I. Tkachova[2] (0000-0002-4605-3429)
Aleksandr V. Maksimenko[2] (0000-0001-9255-3494)
Manfred Thumm[1,3] (0000-0003-1909-3166)
John Jelonnek[1,3] (0000-0002-0531-7600)

[1]Institute for Pulsed Power and Microwave Technology, Karlsruhe Institute of Technology, 76131 Karlsruhe, Germany
[2]National Science Center "Kharkiv Institute of Physics and Technology", 61108 Kharkiv, Ukraine
[3]Institute of Radio Frequency Engineering and Electronics, Karlsruhe Institute of Technology, 76131 Karlsruhe, Germany

Corresponding author: Vitalii I. Shcherbinin (vshch@ukr.net)

Abstract Using a simplified approach, a self-consistent modeling of beam-wave interaction in a complex cavity is performed to evaluate the performance of the complex-cavity second-harmonic 0.4-THz gyrotron developed at the University of Fukui. For this gyrotron, the quantitative analysis of an adverse effect of small manufacturing errors of the complex cavity on mode selection, output power and output mode purity is done. To improve the robustness of gyrotron operation to manufacturing errors, a novel complex cavity formed by coupled smooth-walled and corrugated cylindrical resonators is considered. The novel cavity is a hybrid between conventional cylindrical and standard complex cavities, and therefore offers the benefit of a tradeoff between engineering tolerance and mode selection.

Keywords terahertz radiation, gyrotron, cyclotron harmonics, complex cavity, mode selection, corrugations

Statements and Declarations

Funding Partial financial support was received from the Alexander von Humboldt Foundation and the National Academy of Sciences of Ukraine.

Financial interests The authors declare they have no financial interests.

Non-financial interests Author Manfred Thumm is a member of the Editorial Advisory Board of the JIMTW.

Ethics approval Not applicable

Consent to participate Not applicable

Consent for publication Not applicable

Availability of data and material Data are available from the authors upon reasonable request.

Code availability Not applicable

Authors' contributions All authors contributed to the study conception and design. Material preparation, data collection and analysis were performed by Vitalii I. Shcherbinin. The first draft of the manuscript was written by Vitalii I. Shcherbinin and all authors commented on previous versions of the manuscript. All authors read and approved the final manuscript.

Novel complex cavity for second-harmonic subterahertz gyrotrons: a tradeoff between engineering tolerance and mode selection

Vitalii I. Shcherbinin[1,2*], Tetiana I. Tkachova[2], Aleksandr V. Maksimenko[2], Manfred Thumm[1,3], and John Jelonnek[1,3]

[1]*Institute for Pulsed Power and Microwave Technology, Karlsruhe Institute of Technology, 76131 Karlsruhe, Germany*
[2]*National Science Center "Kharkiv Institute of Physics and Technology", 61108 Kharkiv, Ukraine*
[3]*Institute of Radio Frequency Engineering and Electronics, Karlsruhe Institute of Technology, 76131 Karlsruhe, Germany*

Abstract

Using a simplified approach, a self-consistent modeling of beam-wave interaction in a complex cavity is performed to evaluate the performance of the complex-cavity second-harmonic 0.4-THz gyrotron developed at the University of Fukui. For this gyrotron, the quantitative analysis of an adverse effect of small manufacturing errors of the complex cavity on mode selection, output power and output mode purity is done. To improve the robustness of gyrotron operation to manufacturing errors, a novel complex cavity formed by coupled smooth-walled and corrugated cylindrical resonators is considered. The novel cavity is a hybrid between conventional cylindrical and standard complex cavities, and therefore offers the benefit of a tradeoff between engineering tolerance and mode selection.

Keywords terahertz radiation, gyrotron, cyclotron harmonics, complex cavity, mode selection, corrugations

1. Introduction

Second-harmonic gyrotrons show a capacity for producing high-power continuous-wave radiation up to 1 THz frequency with currently available superconducting magnets [1], and thus can open up new possibilities in various scientific and technological areas today [2].

In second-harmonic gyrotrons, the first major problem facing the designer is the mode competition [3-6], which is posed by the first-harmonic modes of conventional cylindrical cavities. A traditional method to avoid mode competition is to reduce the cavity radius, thereby increasing frequency separation between operating and competing modes. This method has three main shortcomings. First, modern manufacturing technology has a lower limit on cavity diameter of about few millimeters for reasonable dimensional tolerance [7-12]. Second, the smaller is the cavity radius, the higher is the sensitivity of gyrotron operation to manufacturing errors and cavity alignment. Third, miniaturization of a metal cavity enlarges Ohmic losses, resulting in increased thermal loading of the cavity wall and degradation of gyrotron efficiency [6, 12, 14]. These shortcomings become more and more critical with increasing gyrotron frequency. Thus, in the terahertz frequency band, the potentialities of the traditional method of mode selection in second-harmonic gyrotrons will eventually be exhausted.

Improved mode selection can be achieved in complex-shaped cylindrical cavities [15-18] and coaxial cavities [19-23], which are designed to selectively discriminate against the first-harmonic competing modes. Among the complex-shaped cavities the best known is the complex cavity [24]. Its potential advantage is the ability to efficiently suppress all competing modes, regardless of their axial wavenumbers, caustic radii and other characteristics. The complex cavity consists of two jointed cylindrical resonators, which are specially sized to provide coupling between two selected TE modes forming an operating mode with high diffractive quality factor. Unlike the operating mode, competing modes undergo reflection from the junction between the two resonators. Because of this, the length of beam interaction with competing modes decreases and their diffraction losses increase. In theory, this causes the beneficial effect of selective increase in starting currents of all competing modes.

Complex-cavity gyrotrons have been the subject of intensive theoretical [25-29] and experimental [30-35] investigations in 1980s. The emphasis has been placed on the first-harmonic gyrotrons for thermonuclear fusion applications. Despite some progress, it soon became apparent that the disadvantages of complex cavities outweigh the advantages. These disadvantages include high sensitivity to manufacturing errors and reduced output mode purity [36]. That is why the above-mentioned studies have culminated in the abandonment of complex cavities for fusion-relevant first-harmonic gyrotrons in favor of conventional cylindrical cavities.

There are several reasons explaining a rebirth of interest in complex-cavity gyrotrons. First, current technological advances enable precise cavity manufacturing to tolerances of about 1 μm. Second, the mode-selection capabilities of complex cavities look very attractive for use in high-harmonic gyrotrons. Third, for some applications, high mode purity of outgoing radiation is of no critical importance.

A frequency-tunable second-harmonic 0.4-THz gyrotron with complex cavity has been recently developed at the Research Center for Development of Far-Infrared Region, University of Fukui (FIR-UF) [37]. However, despite a precise cavity manufacturing, no excitation of the operating second-harmonic mode was experimentally observed because of severe mode competition with first-harmonic modes [38]. The possible reason is the remaining small errors in cavity dimensions. As indicated in [39, 40], such errors prevent the formation of the high-Q operating mode of the second-harmonic 0.4-THz gyrotron of FIR-UF and lead to increased starting current of this mode. Theoretical investigations of [39,

* vshch@ukr.net

40], however, were done in the fixed-field approximation and therefore can give only qualitative insight into factors affecting mode selection in a complex gyrotron cavity. The quantitative analysis of performance of the frequency-tunable second-harmonic 0.4-THz gyrotron requires self-consistent modeling of beam-wave interaction in the complex cavity. The first aim of this study is to perform such an analysis.

The second aim is to consider a novel complex cavity, which is designed to provide efficient suppression of competing modes, together with improved robustness against manufacturing errors. The novel cavity consists of jointed smooth-walled and corrugated cylindrical resonators of the same radius. The depth and number of periodic longitudinal corrugations have to be properly chosen to ensure the strongest coupling of two selected radial TE modes supported by the jointed resonators and to avoid coupling of these modes with spurious azimuthal modes. Clearly, as the width of corrugations vanishes, the novel complex cavity turns into the conventional cylindrical cavity. The known benefits of the cylindrical cavity are high interaction strength, high purity of outgoing radiation and low sensitivity to manufacturing errors. As the width of the wall corrugations approaches the period, the novel complex cavity acts as standard complex cavity, which is superior to a cylindrical cavity in mode selection. Thus, in the novel cavity, a tradeoff between properties of conventional cylindrical and standard complex cavities can be reached.

2. Theoretical approach

Consider an interaction between a helical electron beam and a mode of a complex metal cavity with a single cavity step, which is a junction between two uniaxial cavity sections of different transverse cross-section. The cavity mode has the angular frequency ω. In coordinates $\{\mathbf{r}_\perp, z\}$, the transverse field of this mode can be expanded in terms of orthogonal normal (waveguide) modes as [25-28, 40]

$$\mathbf{E}_\perp = \sum_n V_n(z)\mathbf{e}_{\perp n}(\mathbf{r}_\perp)$$
$$\mathbf{H}_\perp = \sum_n I_n(z)\mathbf{h}_{\perp n}(\mathbf{r}_\perp)$$

where $V_n(z)$ and $I_n(z)$ are the amplitudes of the transverse electric $\mathbf{e}_{\perp n}(\mathbf{r}_\perp)$ and transverse magnetic $\mathbf{h}_{\perp n}(\mathbf{r}_\perp)$ fields of the n-th normal mode, and the field factor of the form $\exp(-i\omega t)$ is assumed and omitted in the following. Note that the normal modes of a hollow metal waveguide with finite wall conductivity are (quasi-) TE and (quasi-) TM modes.

To investigate coupling of normal modes in a hollow complex cavity we follow a simplified approach [27] and adapt it to normal modes of an impedance (imperfectly conducting) cavity [14, 41]. This approach is based on the following assumptions:

- Among normal modes of the cavity, only a near-cutoff TE mode interacts with an electron beam. This is due to the fact that far-from-cutoff modes are out of resonance with the electron beam. Moreover, below-cutoff modes are evanescent modes, while propagating far-from-cutoff modes have weak coupling with the electron beam, provided that the beam is positioned close to the caustic radius of the near-cutoff TE mode. Before and after the cavity step, this near-cutoff mode can feature different radial indices n and is governed by widely used system of differential equations [14, 27, 42, 43], which are known as gyrotron equations. Note that these equations can be applied to various types of cavities, including dielectric-loaded [22, 44, 45] and corrugated cavities [46].

- Mode conversion in weakly tapered sections of the cavity is negligible. This assumption is known to be justified [47-50]. Besides, the tapering angles of the sections are assumed to be small enough to have only a minor effect on spurious far-from-cutoff modes. Under this assumption, these modes leak out of the input and output cavity ends without reflection from tapered sections of the cavity.

- Mode conversion takes place at the cavity step. In this plane, the amplitudes of near-cutoff TE mode and far-from-cutoff modes are found by the mode-matching technique [27, 28, 45, 51-54].

Thus, in brief, we combine the single-mode gyrotron equations with the mode-matching technique. This approach provides clear insight into the effect of mode conversion induced by the cavity step on gyrotron performance and is rather fast, even though hundreds of coupled normal modes are taken into account. It can be used for numerous simulations required for cavity design and optimization studies.

It should be noted that, in principle, one can use the same basic idea to develop a more rigorous treatment, in which the mode-matching technique is combined with the generalized telegrapher's equations [55-57]. Such a treatment is free from above assumptions. At the same time, it is associated with time-consuming computations and therefore is best suited for use as a checking tool. The development of such a tool is now under way for further research.

3. Conventional cylindrical cavity

Our interest is in the performance of a second-harmonic 0.4-THz gyrotron powered by the electron beam with current $I_b = 0.3$ A, voltage $V_b = 15$ kV, radius $r_b = 0.916$ mm, and pitch factor $\alpha = 1.5$. As a benchmark, we first consider the gyrotron operated in the $TE_{8,4}$ mode of a conventional cylindrical cavity (Fig. 1a), which is made from copper. The realistic RF conductivity of copper is assumed to be 2.9×10^7 S/m. The cavity has the radius $R = 2.588$ mm and length $L = 35$ mm, and is connected to input and output sections with tapering angles $\theta_{in} = 2°$ and $\theta_{out} = 3°$, respectively. The

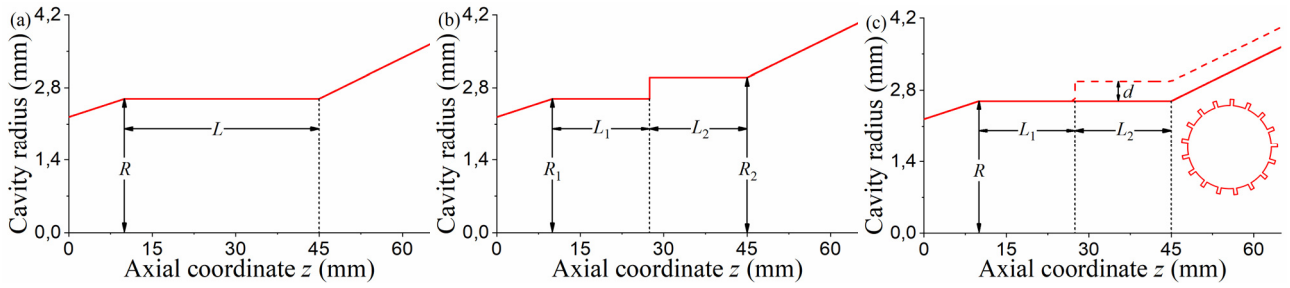

Fig. 1 Design of (a) conventional cavity, (b) standard complex cavity [37, 38], and (c) novel complex cavity, where $R = R_1 = 2.588$ mm, $R_2 = 2.9974$ mm, $L = L_1 + L_2$, $L_1 = L_2 = 17.5$ mm, $d = 0.3833$ mm, $\vartheta_{in} = 2°$, and $\vartheta_{out} = 3°$

cold diffractive Q_{dif} and ohmic Q_{ohm} quality factors of the $TE_{8,4,q}$ mode are $193910/q^2$ and 14870, respectively. For simplicity, a spread in velocity, energy and injection radius of beam electrons is neglected.

Fig. 2a shows the output power of the second-harmonic 0.4-THz gyrotron in the single-mode regime as a function of the operating magnetic field B_0. It is seen that the conventional-cavity gyrotron can theoretically produce radiation in a wide frequency band with output power ranging from ten to hundred of watts. Noteworthy are high ohmic losses in the long cylindrical cavity, which explain a trend toward a decrease of the output power with decrease in both the magnetic field B_0 and axial index q of the $TE_{8,4,q}$ mode.

At the same time, it is highly unlikely that the operating second-harmonic mode could actually be excited by the electron beam in the conventional cavity. The reason is the mode competition. The most dangerous competing mode is the first-harmonic $TE_{5,2}$ mode. As can be seen from Fig. 2b, the starting current of the $TE_{5,2}$ mode lies well below the operating beam current and is generally lower than that of the operating mode. In such a situation, the first-harmonic competing mode presents a barrier to operation of the second-harmonic 0.4-THz gyrotron [5, 6].

4. Complex cavity

To overcome this barrier a standard complex cavity can be used in the second-harmonic 0.4-THz gyrotron. The complex cavity has a structure shown in Fig. 1b and is identical to that of the second-harmonic 0.4-THz gyrotron designed at FIR-UF for operation in the $TE_{8,4}$-$TE_{8,5}$ mode pair [37, 38]. For brevity, this mode pair will be referred to as the "operating mode". The copper cavity consists of two jointed cylindrical resonators of the same length $L_1 = L_2 = 17.5$ mm. The radii $R_1 = 2.588$ mm and $R_2 = 2.9974$ mm of the first and second resonators are adjusted to provide the strongest coupling of the $TE_{8,4}$ and $TE_{8,5}$ modes. For these radii, the fitting condition $\mu_{8,4}/R_1 = \mu_{8,5}/R_2$ is fulfilled to a high accuracy, where $\mu_{8,4}$ and $\mu_{8,5}$ are the eigenvalues of the $TE_{8,4}$ and $TE_{8,5}$ modes, respectively.

Cold-cavity calculations provide an easy way to gain a useful insight into main features of a gyrotron cavity. For this reason, the simplified approach has been adapted to calculate the cold frequency f_c, diffractive Q_{dif}, ohmic Q_{ohm} and total Q_{tot} quality factors of the complex cavity. For the operating mode with lowest diffractive losses, it yields $f_c = 391.46$ GHz, $Q_{dif} = 41050$, $Q_{ohm} = 16300$ and $Q_{tot} = 11670$. Since f_c and Q_{dif} show a decrease with decreasing wall conductivity, the calculated cold characteristics of the complex cavity are found to be in good agreement with published data of [39, 40, 58].

Manufacturing errors of the complex cavity violate the fitting condition and reduce the coupling of the $TE_{8,4}$ and $TE_{8,5}$ modes. For simplicity, we consider a nonzero error δ_R in radius R_2 of the second resonator. This error affects the

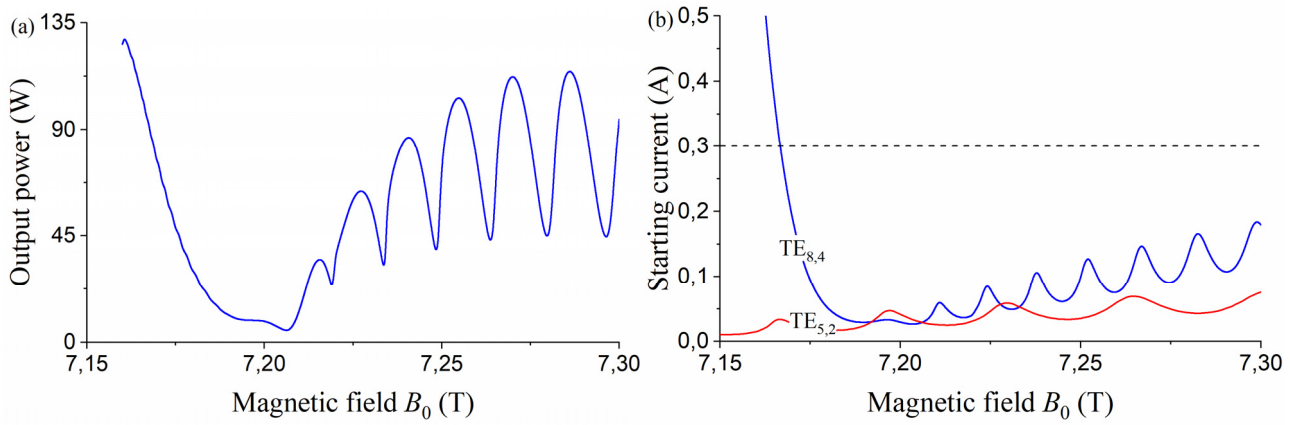

Fig. 2 (a) Output power of the operating $TE_{8,4}$ mode and (b) starting currents of the operating and competing $TE_{5,2}$ modes of the conventional-cavity second-harmonic 0.4-THz gyrotron versus applied magnetic field

frequency and quality factor of the operating mode [39, 40], together with output mode purity η_p and effective cavity length (interaction length)

$$L_{eff} = 2\int_{z_{in}}^{z_{out}} dz\left|\tilde{V}_{4,5}(z)\right|^2,$$

where $\left|\tilde{V}_{4,5}(z)\right|$ is the normalized amplitude of the $TE_{8,4}$-$TE_{8,5}$ mode pair with unit peak value, z_{in} and z_{out} are coordinates of the input and output cavity ends, respectively.

As Fig. 3 suggests, the error δ_R causes a drop in the quality factor (see also the blue curve in Fig. 5b of [39]) and interaction length of the cavity. Because of this, for the operating mode, one can expect an increase of the starting current, which is inversely proportional to $Q_{tot}L_{eff}^2$ [13, 59]. In addition, the error δ_R lowers the output mode purity η_p, resulting in reduced content of the outgoing $TE_{8,5}$ mode in output radiation. The strong effect of δ_R on the operating mode can also be seen in Fig. 4a-4c and Table I. Note that this effect is reduced by a decrease in diffractive quality factor of the complex cavity and therefore is smaller for higher-order axial resonances of the operating mode [39].

Contrary to the operating mode, the competing $TE_{5,2}$ mode is nearly insensitive to the error δ_R. This is because the $TE_{5,2}$ mode is supported by the first resonator of the complex cavity (see Fig. 4d) and therefore is only slightly affected by the radius R_2. The only possible effect of the manufacturing errors on this mode is a frequency shift, which can be induced by the change in radius R_1 of the first resonator. Thus, cold-cavity calculations give a clear indication of reduced benefit of the complex cavity for the second-harmonic 0.4-THz gyrotron due to small manufacturing errors. However, to draw quantitative inferences about this benefit, modeling of the beam-wave interaction in the complex cavity is required.

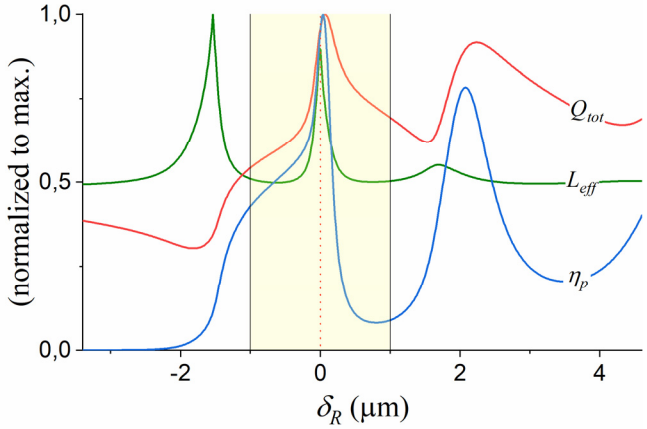

Fig. 3 The dependence of Q_{tot}, L_{eff} and η_p on the error δ_R. The peak values of Q_{tot}, L_{eff} and η_p are 12180, 40.7 mm and 90.3 %, respectively

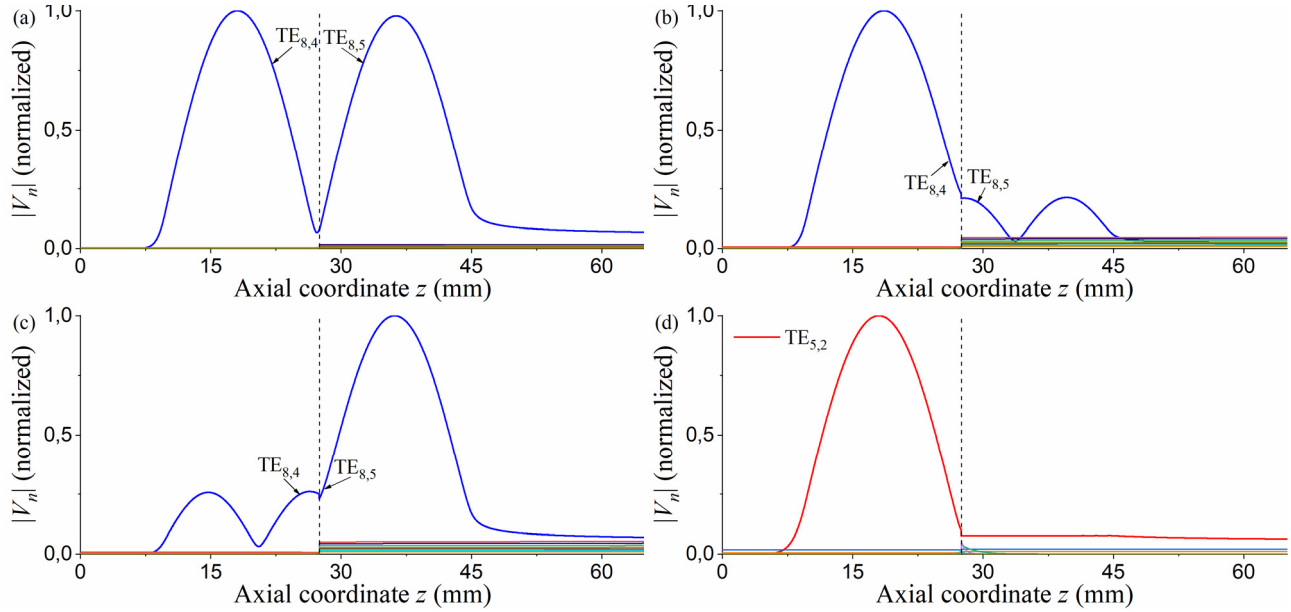

Fig. 4 Cold field profiles of the operating mode for (a) $\delta_R = 0$, (b) $\delta_R = +1$ μm, and (c) $\delta_R = -1$ μm, and (d) of the competing mode for $\delta_R = 0$ inside complex cavity. Cold characteristics of these modes are listed in Table I

Table I
Cold characteristics of modes shown in Fig. 4

Case	f_c(GHz)	Q_{dif}	Q_{ohm}	Q_{tot}	L_{eff} (mm)	η_p (%)
(a)	391.460	41050	16300	11670	36.4	85.9
(b)	391.451	18830	15320	8450	20.5	8.0
(c)	391.586	10380	18260	6620	20.8	38.7
(d)	194.089	11282	9560	5180	20.0	84.0

Fig. 5a shows starting currents of the operating mode and competing first-harmonic $TE_{5,2}$ mode of the second-harmonic 0.4-THz gyrotron with nominal complex cavity ($\delta_R = 0$). It is seen that the starting current of the operating mode of the complex cavity varies sharply with applied magnetic field B_0 and features reduced number of local minima, which correspond to even axial resonances of the operating mode. The cavity step initiates an increase in starting currents of both the operating and competing modes. It is seen from Figs. 2b and 5a that this increase is larger for the competing $TE_{5,2}$ mode. Thus, as expected, the complex cavity is superior to the cylindrical cavity in mode selection for the second-harmonic 0.4-THz gyrotron.

At the same time, mode selection in the complex cavity is adversely affected by manufacturing errors. For $\delta_R = \pm 1$ μm [38], this is also seen in Fig. 5a. As expected, an error δ_R generally enlarges the starting current of the operating mode. A larger increase is observed for starting currents of lower axial modes. Despite this, the error $\delta_R = \pm 1$ μm on its own does not completely rule out the excitation of the operating second-harmonic mode of the complex-cavity 0.4-THz gyrotron. As is seen from Fig. 5a, the possible excitation zone is located close to $B_0 = 7.21$ T. This is inconsistent with experimental observations in [38]. Considering no additional factors, no experimental evidence of the operating mode of the second-harmonic 0.4-THz gyrotron can be explained by larger manufacturing errors. For $B_0 = 7.21$ T, the influence of δ_R on the starting current of the operating mode is shown in Fig. 5b. It is seen that generation of the operating mode is forbidden for $I_b = 0.3$ A and error δ_R larger than +3 μm.

Additional calculations have been done to evaluate the output power of the second-harmonic 0.4-THz gyrotron with complex cavity. The calculated data are shown in Fig. 6a. It is interesting, but not surprising [13], that the complex-cavity gyrotron can outperform the conventional-cavity counterpart in peak output power. This is because of lower ohmic losses

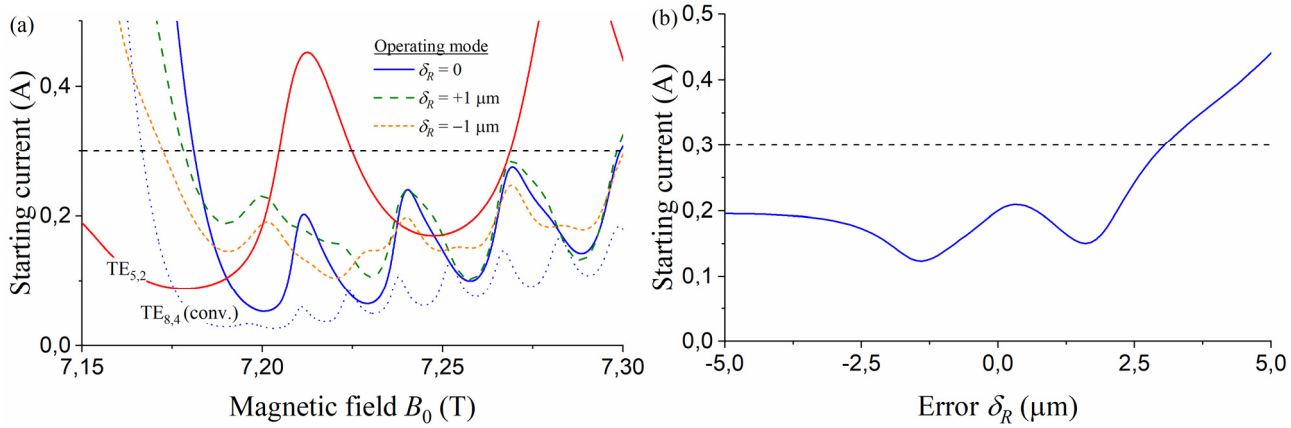

Fig. 5 (a) Starting currents of the operating and competing modes of the complex-cavity second-harmonic 0.4-THz gyrotron versus the magnetic field B_0 for different δ_R, and (b) influence of the manufacturing error δ_R on the starting current of the operating mode for $B_0 = 7.21$ T

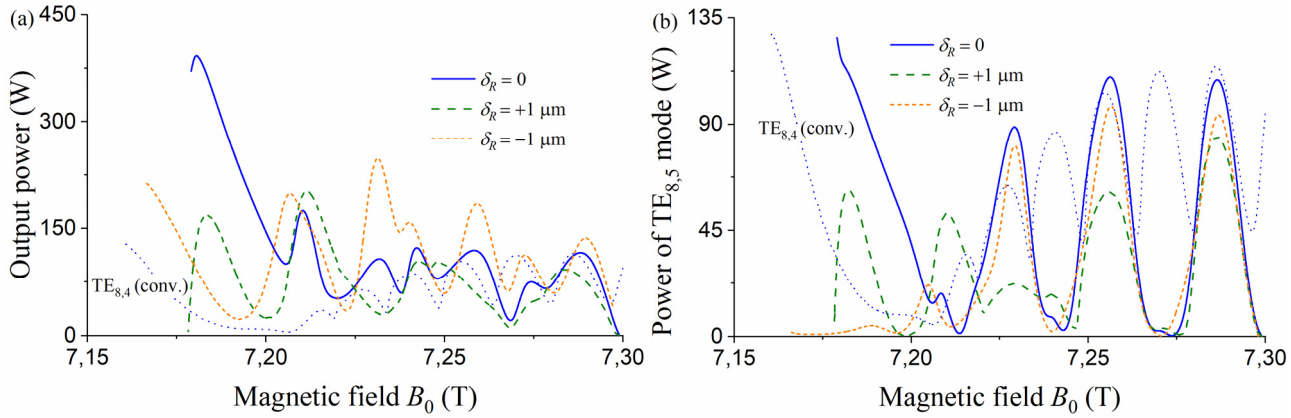

Fig. 6 (a) Output power of the complex-cavity second-harmonic 0.4-THz gyrotron and (b) power of the outgoing $TE_{8,5}$ mode of the complex cavity for different δ_R

in the complex cavity, which is characterized by the reduced diffractive quality factor. However, as is seen from Fig. 6a, the peak output power of the second-harmonic 0.4-THz gyrotron is drastically reduced by an increasing manufacturing error δ_R of the complex cavity.

It is significant that the output mode purity of the complex-cavity 0.4-THz gyrotron is strongly dependent on the operating magnetic field. For the outgoing $TE_{8,5}$ mode, this leads to sharp power variation along the frequency tuning band (Fig. 6b). The mode purity reaches 99% for high-order axial resonances of the operating mode and can drop below 1% for transient states between resonances, even if the assumed error δ_R is set to zero. A rapid variation of the output mode purity with operating frequency makes the design of an output mode converter for the frequency-tunable complex-cavity gyrotron very challenging. Here, it should be mentioned that an intermediate slot (stub) between the two coupled resonators of a complex cavity can reduce conversion of the operating mode to spurious normal modes and thus furnishes a way of improving the output mode purity [58]. However, its effect on the performance of the complex-cavity gyrotron is beyond the scope of this study and call for further investigation, which requires modification of the above-described theoretical approach of [27].

5. Novel complex cavity

Let us now consider a novel complex cavity as a tradeoff between cylindrical and standard complex cavities for the second-harmonic 0.4-THz gyrotron. In this cavity, a smooth-walled cylindrical resonator is jointed to a corrugated cylindrical resonator of the same radius $R = 2.588$ mm and length $L_1 = L_2 = 17.5$ mm (Fig. 1c). The depth d of longitudinal corrugations is set close to a half vacuum wavelength at the operating frequency and equals 0.3833 mm. For such corrugation depth, the ohmic losses in a metal corrugated wall are moderate [46, 54, 60-63]. More importantly, in this case, the operating normal TE modes supported by the smooth-walled and corrugated cylindrical resonators have nearly equal eigenvalues and features the strongest coupling [46, 54, 63].

The novel cavity exhibits properties of cylindrical or standard complex cavities depending on the width w and number

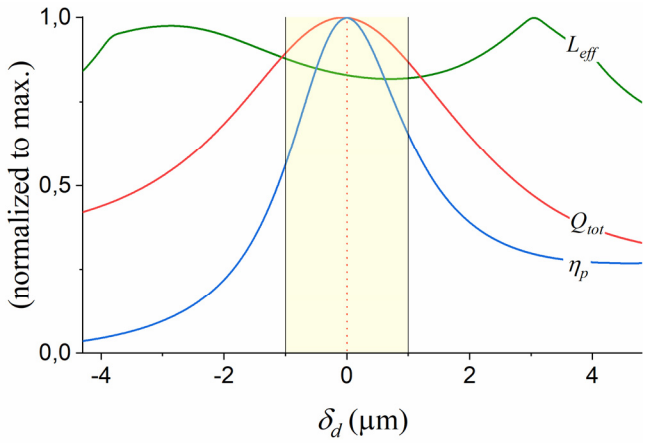

Fig. 7 Cold characteristic of the novel complex cavity as functions of the error δ_d. The peak values of Q_{tot}, L_{eff} and η_p are 10280, 40 mm and 90.8 %, respectively

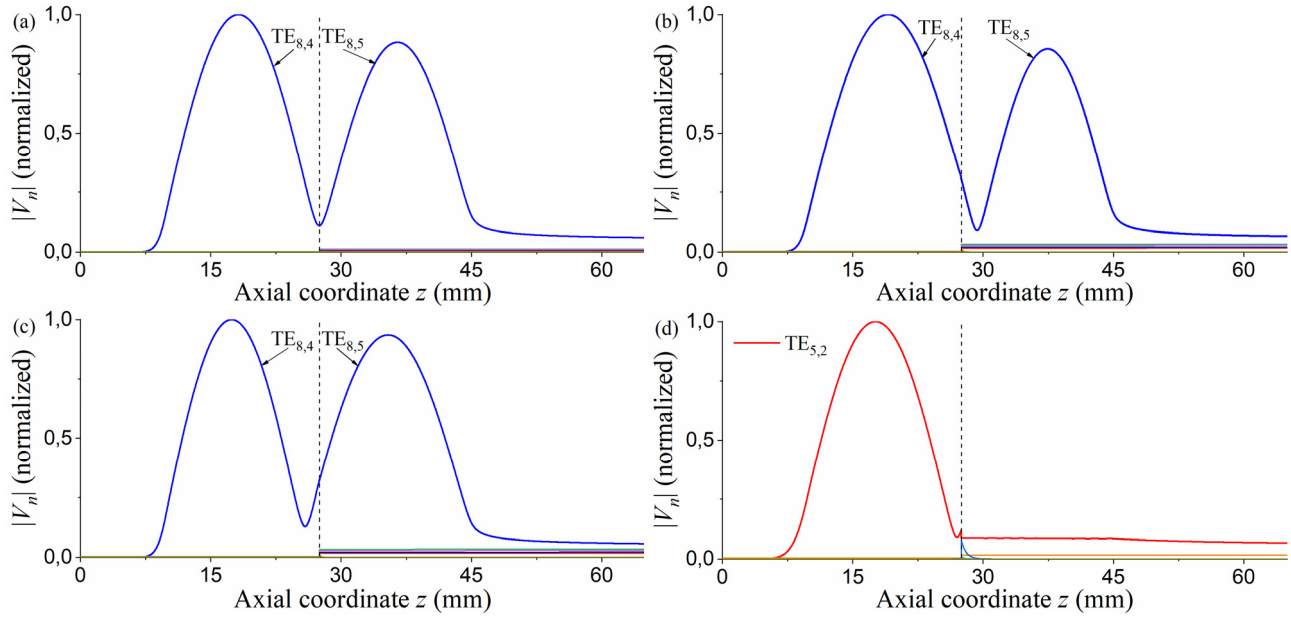

Fig. 8 Cold field profiles of the operating mode for (a) $\delta_d = 0$, (b) $\delta_d = +1$ μm, and (c) $\delta_d = -1$ μm, and (d) of the competing mode for $\delta_d = 0$ inside novel complex cavity. The cold characteristics of these modes are listed in Table II

Table II
Cold characteristics of modes shown in Fig. 8

Case	f_c(GHz)	Q_{dif}	Q_{ohm}	Q_{tot}	L_{eff} (mm)	η_p (%)
(a)	391.458	48950	13000	10280	33.2	90.8
(b)	391.444	27130	13290	8920	32.9	59.3
(c)	391.474	32650	12800	9200	35.2	51.1
(d)	194.105	11350	11390	5700	19.4	93.6

N of corrugations. In deciding on specific values of w and N, the following tendencies should be taken into account. Decrease in the number of corrugations leads to reduced ohmic losses in a corrugated wall [46, 62, 63], but can initiate undesirable coupling of the operating mode with spurious azimuthal modes [46, 61-63]. Decrease in the width of corrugations improves the robustness of the cavity characteristics against manufacturing errors, but reduces the mode-selection capability and can add complexity to the manufacturing process. All things considered, we arrive at $w = 0.2$ mm and $N = 17$. Using these parameters, we obtain $f_c = 391.458$ GHz, $Q_{dif} = 48950$, $Q_{ohm} = 13000$ and $Q_{tot} = 10280$ for the high-Q operating mode of the novel complex cavity.

The main factor affecting mode coupling in the designed cavity is the depth of the corrugations. Therefore, we next assume an error δ_d in the corrugation depth d. Figs. 7, 8a-8c and Table II show the effect of δ_d on cold characteristics of the novel complex cavity. As is seen from Figs. 3 and 7, these characteristics are less sensitive to manufacturing errors than those of the standard cavity. In addition, the novel cavity is characterized by reduced interaction length and diffractive quality factor of the competing $TE_{5,2}$ mode (Fig. 8d) and therefore is expected to favor suppression of this mode.

Fig. 9a shows starting currents of the operating and competing modes of the second-harmonic 0.4-THz gyrotron with novel complex cavity. It is clearly seen that, compared to a standard complex cavity, the novel cavity is characterized by lower starting current of the operating mode and therefore provides better discrimination against the competing $TE_{5,2}$ mode. Moreover, as expected, this cavity shows better robustness against manufacturing errors than the standard one. This can also be seen in Fig. 9b. It is evident that, in the novel cavity, the operating mode can be generated for errors ± 10 μm in both depth and width of corrugations. Such a tolerance is fully met by modern manufacturing techniques.

Fig. 10a shows the output power of the second-harmonic 0.4-THz gyrotron utilizing the novel complex cavity. The

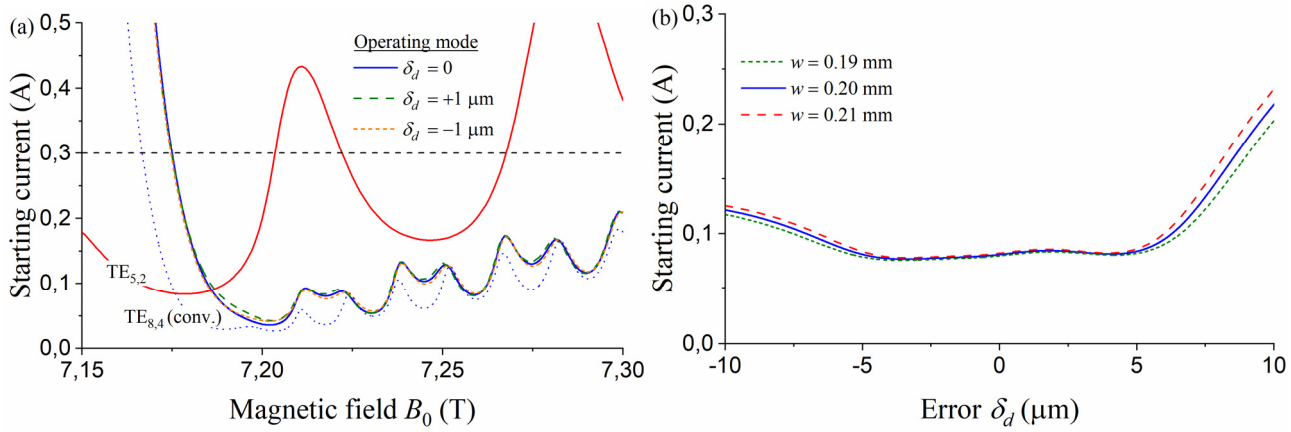

Fig. 9 (a) Starting currents of the operating and competing modes of the second-harmonic 0.4-THz gyrotron with novel complex cavity versus the magnetic field B_0 for different δ_d, and (b) influence of the manufacturing errors in depth and width of corrugations on the starting current of the operating mode for $B_0 = 7.21$ T

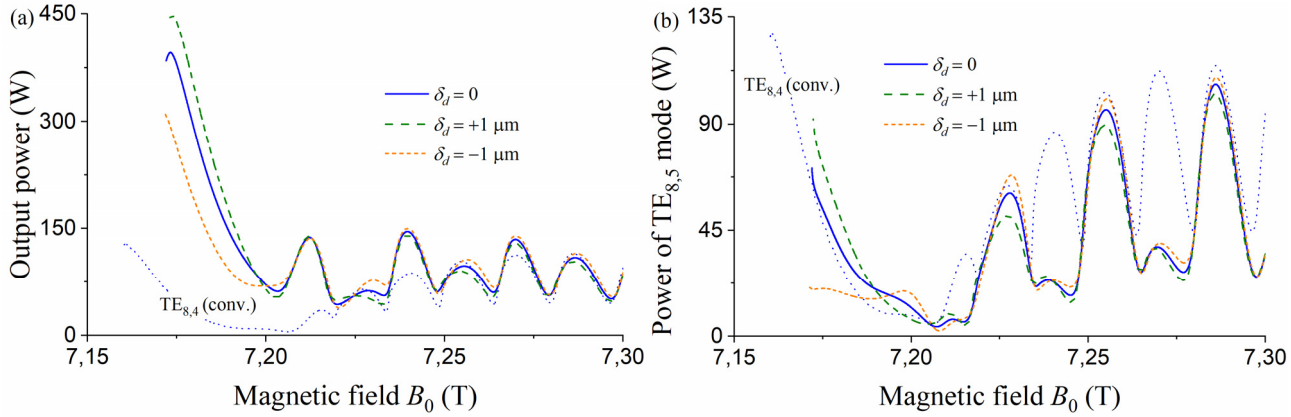

Fig. 10 (a) Output power of the second-harmonic 0.4-THz gyrotron with novel complex cavity and (b) power of the outgoing $TE_{8,5}$ mode of the novel cavity for different δ_d

output power varies smoother along the operating range and is less affected by errors than that of the standard complex-cavity gyrotron (Fig. 6a). The only weakness of the novel cavity is a frequency-dependent mode content of the output radiation (Fig. 10b). The mode purity is somewhat affected by the error δ_d and is around 99% and 25% for high-order even axial resonances and transient states between them, respectively. A way of improving the output mode purity is to reduce the width w of corrugations to minimum, which on the one hand must be reached by available manufacturing technology and on the other hand can still offer efficient suppression of competing modes.

6. Conclusions

A fast simplified approach has been used to critically analyze a practical benefit of complex cavities for second-harmonic subterahertz gyrotrons. For clarity, a comparison between the performance of the complex-cavity and cylindrical-cavity gyrotrons has been presented. As a concrete example, the complex and cylindrical cavities for the frequency-tunable second-harmonic 0.4-THz gyrotron of FIR-UF have been considered. It has been shown that the complex cavity enables generation of the desired second-harmonic operating mode (mode pair), which suffers from severe mode competition in a cylindrical cavity. At the same time, the complex-cavity gyrotron exhibits a sharp power variation along the frequency tuning band and reduced output mode purity, which can range from 1 to 99 % depending on frequency of the operating mode. Moreover, the performance of the complex-cavity second-harmonic 0.4-THz gyrotron is impaired by small manufacturing errors in cavity radius. Such errors have only a minor effect on the competing modes, which are supported by either of two resonators of the complex cavity. The strongest effect has been observed for the lowest axial operating mode, which shows more than 100% increase in starting current and more than 100% decrease in output power for the manufacturing error of 1 μm. A novel complex cavity formed by coupled smooth-walled and corrugated cylindrical resonators has been considered as a design solution intended to improve the performance of the second-harmonic 0.4-THz gyrotron. The longitudinal wall corrugations have been designed to ensure the following characteristics: the strongest coupling of the operating radial modes of smooth-walled and corrugated resonators, moderate ohmic losses of the operating mode, no coupling of the operating mode to spurious azimuthal modes, and good robustness of gyrotron performance to manufacturing errors in both depth and width of corrugations. It has been found that the novel cavity is superior to both cylindrical and standard complex cavities in mode selection. In addition, the output power of the second-harmonic gyrotron with the novel cavity varies smoother with operating frequency and is less affected by manufacturing errors than that of the standard complex-cavity gyrotron. However, similar to the standard cavity, the novel complex cavity has been shown to have the frequency-dependent output mode purity, which can present a serious handicap to the design of the output mode converter for the frequency-tunable 0.4-THz gyrotron.

Acknowledgements

The work of V.I. Shcherbinin was supported by the Alexander von Humboldt Foundation via the Georg Forster Research Fellowship for Experienced Researchers and Philipp Schwartz Initiative for Researchers at Risk. The work of T.I. Tkachova and A.V. Maksimenko was supported by the Grant of the National Academy of Sciences of Ukraine to Research Laboratories/Groups of Young Scientists of the National Academy of Sciences of Ukraine for Conducting Research in Priority Areas of Science and Technology in 2022-2023.

References

1. M. Thumm, J. Infrared Millim. Terahertz Waves (2020) https://doi.org/10.1007/s10762-019-00631-y
2. S. Sabchevski, M. Glyavin, S. Mitsudo, Y. Tatematsu, T. Idehara, J. Infrared Millim. Terahertz Waves (2021) https://doi.org/10.1007/s10762-021-00804-8
3. T. Idehara, T. Tatsukawa, I. Ogawa, T. Mori, H. Tanabe, S. Wada, G. F. Brand, M. H. Brennan, Appl. Phys. Lett. (1991) https://doi.org/10.1063/1.105135
4. G.F. Brand, T. Idehara, T. Tatsukawa, I. Ogawa, Int. J. Electron. (1992) https://doi.org/10.1080/00207219208925612
5. V.L. Bratman, A.E. Fedotov, T. Idehara, Int. J. Infrared Millim. Waves (2001) https://doi.org/10.1023/A:1015030405179
6. S.H. Kao, C.C. Chiu, K.R. Chu, Phys. Plasmas (2012) https://doi.org/10.1063/1.3684663
7. A.C. Torrezan, S.T. Han, I. Mastovsky, M.A. Shapiro, J.R. Sirigiri, R.J. Temkin, A.B. Barnes, R.G. Griffin, IEEE Trans. Plasma Sci. (2010) https://doi.org/10.1109/TPS.2010.2046617
8. T. Idehara, I. Ogawa, La Agusu, T. Kanamaki, S. Mitsudo, T. Saito, T. Fujiwara, H. Takahashi, Int. J. Infrared Millim. Waves (2010) https://doi.org/10.1007/s10762-010-9643-y
9. A.C. Torrezan, M.A. Shapiro, J.R. Sirigiri, R.J. Temkin, R.G. Griffin, IEEE Trans. Electron Devices (2011) https://doi.org/10.1109/TED.2011.2148721
10. T. Idehara, Y. Tatematsu, Y. Yamaguchi, E.M. Khutoryan, A.N. Kuleshov, K. Ueda, Y. Matsuki, T. Fujiwara, J. Infrared Millim. Terahertz Waves (2015) https://doi.org/10.1007/s10762-015-0150-z
11. S K. Jawla, R.G. Griffin, I.A. Mastovsky, M.A. Shapiro, R.J. Temkin, IEEE Trans. Electron Devices (2020) https://doi.org/10.1109/TED.2019.2953658
12. M.Yu. Glyavin, A.N. Kuftin, M.V. Morozkin, M.D. Proyavin, A.P. Fokin, A.V. Chirkov, V.N. Manuilov, A.S. Sedov, E.A. Soluyanova, D.I. Sobolev, E.M. Tai, A.I. Tsvetkov, A.G. Luchinin, S.Yu. Kornishin, G.G. Denisov, IEEE Electron Device Lett. (2021) https://doi.org/10.1109/LED.2021.3113022

13. M.Y. Glyavin, N.A. Zavolskiy, A.S. Sedov, G.S. Nusinovich, Phys. Plasmas (2013) https://doi.org/10.1063/1.4791663
14. V.I. Shcherbinin, A.V. Hlushchenko, A.V. Maksimenko, V.I. Tkachenko (2017) https://doi.org/10.1109/TED.2017.2730252.
15. S. Spira-Hakkarainen, K.E. Kreischer, R.J. Temkin, IEEE Trans. Plasma Sci. (1990) https://doi.org/10.1109/27.55903
16. I.V. Bandurkin, Yu.K. Kalynov, A.V. Savilov, Phys. Plasmas (2013) https://doi.org/10.1063/1.4775083
17. Yu.S. Oparina, A.V. Savilov, J. Infrared Millim. Terahertz Waves (2018) https://doi.org/10.1007/s10762-018-0499-x
18. I.V. Bandurkin, M.Y. Glyavin, A.E. Fedotov, A.P. Fokin, M. Fukunari, I.V. Osharin, A.V. Savilov, D.Y. Shchegolkov, Y. Tatematsu, IEEE Trans. Electron Devices (2022) https://doi.org/10.1109/TED.2022.3142657
19. K.A. Avramides, C.T. Iatrou, J.L. Vomvoridis, IEEE Trans. Plasma Sci. (2004) https://doi.org/10.1109/TPS.2004.828781
20. V.I. Shcherbinin, V.I. Tkachenko, K.A. Avramidis, J. Jelonnek, IEEE Trans. Electron Devices (2019) https://doi.org/10.1109/TED.2019.2944647
21. V.I. Shcherbinin, Y.K. Moskvitina, K.A. Avramidis, J. Jelonnek, IEEE Trans. Electron Devices (2020) https://doi.org/10.1109/TED.2020.2996179
22. V.I. Shcherbinin, K.A. Avramidis, M. Thumm, J. Jelonnek, J. Infrared Millim. Terahertz Waves (2021) https://doi.org/10.1007/s10762-020-00760-9
23. V.I. Shcherbinin, IEEE Trans. Electron Devices (2021) https://doi.org/10.1109/TED.2021.3090348
24. S.A. Malygin, V.G. Pavel'ev, Sh.E. Tsimring, in Gyrotrons: Collected Papers, ed. by V. A. Flyagin, G. S. Nusinovich, V. K. Yulpatov, N. A. Gorodetskaya (USSR Academy of Science, Institute of Applied Physics, Gorky, 1980), p. 78 (in Russian)
25. S.A. Malygin, V.G. Pavel'ev, Sh.E. Tsimring, Radiophys. Quantum Electron. (1983) https://doi.org/10.1007/BF01039282
26. V.G. Pavel'ev, Sh.E. Tsimring, V.E. Zapevalov, Int. J. Electron. (1987) https://doi.org/10.1080/00207218708939142
27. A.W. Flifiet, R.C. Lee, M.E. Read, Int. J. Electron. (1988) https://doi.org/10.1080/00207218808945229
28. O. Dumbrajs, E. Borie, Int. J. Electron. (1988) https://doi.org/10.1080/00207218808945230
29. E. Borie, B. Jödicke, H. Wenzelburger, O. Dumbrajs, Int. J. Electron. (1988) https://doi.org/10.1080/00207218808962788
30. A.V. Gaponov, V.A. Flyagin, A.L. Goldenberg, G.S. Nusinovich, Sh.E. Tsimring, V.G. Usov, S.N. Vlasov, Int. J. Electron. (1981) https://doi.org/10.1080/00207218108901338
31. Y. Carmel, K.R. Chu, M. Read, A.K. Ganguly, D. Dialetis, R. Seeley, J.S. Levine, V.L. Granatstein, Phys. Rev. Lett. (1983) https://doi.org/10.1103/PhysRevLett.50.112
32. K.L. Felch, R. Bier, L. Fox, H. Huey, L. Ives, H. Jory, N. Lopez, J. Manca, J. Shively, S. Spang, Int. J. Electron. (1984) https://doi.org/10.1080/00207218408938968
33. V.E. Zapevalov, S.A. Malygin, V.G. Pavel'ev, Radiophys. Quantum Electron. (1984) https://doi.org/10.1007/BF01041396
34. G. Mourier, G. Faillon, P. Garin, Int. J. Electron. (1986) https://doi.org/10.1080/00207218608920917
35. S.A. Malygin, Sov. J. Commun. Technol. Electron. 31, 106 (1986)
36. M.V. Kartikeyan, E. Borie, M.K.A. Thumm, Gyrotrons: High Power Microwave and Millimeter Wave Technology (Springer, Berlin, 2004), pp. 41-44
37. Y. Yamaguchi, M. Fukunari, T. Ogura, T. Ueyama, Y. Maeda, K. Takayama, Y. Tatematsu, T. Saito, Proc. 43rd Int. Conf. Infrared Millim. Terahertz Waves (2018) https://doi.org/10.1109/IRMMW-THz.2018.8510274
38. Y. Yamaguchi, T. Ogura, T. Ueyama, Y. Maeda, K. Takayama, J. Sasano, M. Fukunari, Y. Tatematsu, T. Saito, IEEE Electron Device Lett. (2020) https://doi.org/10.1109/LED.2020.3000640
39. M.M. Melnikova, A.G. Rozhnev, N.M. Ryskin, Y. Tatematsu, M. Fukunari, Y. Yamaguchi, T. Saito, IEEE Trans. Electron Devices (2017) https://doi.org/10.1109/TED.2017.2764874
40. A.V. Maksimenko, V.I. Shcherbinin, A.V. Hlushchenko, V.I. Tkachenko, K.A. Avramidis, J. Jelonnek, IEEE Trans. Electron Devices (2019) https://doi.org/10.1109/TED.2019.2893888
41. V.I. Shcherbinin, G.I. Zaginaylov, V I. Tkachenko, Problems Atomic Sci. Technol. 4 (98), 89 (2015)
42. V.L. Bratman, M.A Moiseev, M.I. Petelin, R.É. Érm, Radiophys. Quantum Electron. (1973) https://doi.org/10.1007/BF01030898
43. V.A. Flyagin, A.V. Gaponov, M.I. Petelin, V.K. Yulpatov, IEEE Trans. Microwave Theory Tech. (1977) https://doi.org/10.1109/TMTT.1977.1129149
44. C.-H. Du, P.-K. Liu (2010) doi: https://doi.org/10.1063/1.3339935
45. V. I. Shcherbinin, K. A. Avramidis, I. Gr. Pagonakis, M. Thumm, J. Jelonnek, J. Infrared Millim. Terahertz Waves (2021) 10.1007/s10762-021-00814-6.
46. T.I. Tkachova, V.I. Shcherbinin, V.I. Tkachenko, Z.C. Ioannidis, M. Thumm, J. Jelonnek, J. Infrared Millim. Terahertz Waves (2021) https://doi.org/10.1007/s10762-021-00772-z
47. E. Borie, O. Dumbrajs, Int. J. Electron. (1986) https://doi.org/10.1080/00207218608920768
48. G.I. Zaginaylov, V.I. Shcherbinin, K. Schünemann, M. Yu Glyavin, Proc. 8th Int. Kharkiv Symp. Phys. Eng.

Microw. Millim. Submillim. Waves (2013) https://doi.org/10.1109/MSMW.2013.6622127
49. A.V. Maksimenko, G.I. Zaginaylov, V.I. Shcherbinin, Physics of Particles and Nuclei Letters (2015) https://doi.org/10.1134/S1547477115020168
50. A.V. Maksimenko, V.I. Shcherbinin, V.I. Tkachenko, J. Infrared Millim. Terahertz Waves (2019) https://doi.org/10.1007/s10762-019-00589-x
51. J.M. Neilson, P.E. Latham, M. Caplan, W.G. Lawson, IEEE Trans. Microw. Theory Techn. (1989) https://doi.org/10.1109/22.31074
52. Wagner, G. Gantenbein, W. Kasparek, M. Thumm, Int. J. Infrared Millim. Waves (1995) https://doi.org/10.1007/BF02274811
53. V.I. Shcherbinin, G.I. Zaginaylov, V.I. Tkachenko, Problems Atomic Sci. Technol. 6 (106), 255 (2016).
54. V.I. Shcherbinin, V.I. Tkachenko, J. Infrared Millim. Terahertz Waves (2017) https://doi.org/10.1007/s10762-017-0386-x
55. M. Botton, T.M. Antonsen, Jr., B. Levush, K.T. Nguyen, A.N. Vlasov, IEEE Trans. Plasma Sci. (1998) https://doi.org/10.1109/27.700860
56. H. Yong, L. Hongfu, D. Pingzhong, L. Shenggang, IEEE Trans. Plasma Sci. (1998) https://doi.org/10.1109/27.650910
57. A.V. Maksimenko, V.I. Shcherbinin, V.I. Tkachenko, Proc. IEEE Ukr. Microw. Week (2020) https://doi.org/10.1109/UkrMW49653.2020.9252719
58. D. Wagner, M. Thumm, IEEE Trans. Electron Devices (2021) https://doi.org/10.1109/TED.2021.3105955
59. B.G. Danly, R.J. Temkin, Phys. Fluids (1986) https://doi.org/10.1063/1.865446.
60. V.I. Shcherbinin, B.A. Kochetov, A.V. Hlushchenko, V.I. Tkachenko, IEEE Trans. Microw. Theory Techn. (2019) https://doi.org/10.1109/TMTT.2018.2882493
61. T.I. Tkachova, V.I. Shcherbinin, V.I. Tkachenko, Problems Atomic Sci. Technol. 6 (118), 67 (2018)
62. T.I. Tkachova, V.I. Shcherbinin, V.I. Tkachenko, Problems Atomic Sci. Technol. 4 (122), 31 (2019)
63. T.I. Tkachova, V.I. Shcherbinin, V.I. Tkachenko, J. Infrared Millim. Terahertz Waves (2019) https://doi.org/10.1007/s10762-019-00623-y